Available online at www.sciencedirect.com
SCIENCE DIRECT®
Materials Chemistry and Physics 88 (2004) 250–257
MATERIALS CHEMISTRY AND PHYSICS
www.elsevier.com/locate/matchemphys

Effect of thickness on the properties of vacuum deposited $Cd_{0.75}Sn_{0.25}Se$ mixed chalcogenide thin films

D. Pathinettam Padiyan [a,*], A. Marikani [b], K.R. Murali [c]

[a] *Department of Physics, Manonmaniam Sundaranar University, Tirunelveli 627 012, India*
[b] *Mepco Schlenk Engineering College, Virudhunagar 626 005, Tamil Nadu, India*
[c] *Central Electrochemical Research Institute, Karaikudi 630 006, Tamil Nadu India*

Received 13 May 2003; received in revised form 25 July 2003; accepted 23 September 2003

Abstract

Polycrystalline $Cd_{0.75}Sn_{0.25}Se$ thin films with different thicknesses were deposited by single source on glass substrates maintained at room temperature. The lattice parameters for synthesized $Cd_{0.75}Sn_{0.25}Se$ powder are determined. The structural, electrical, optical and photoelectrical properties of these films were studied and are reported.
© 2003 Elsevier B.V. All rights reserved.

Keywords: Semiconductor; Thin films; Electrical properties; Vapour deposition; Optical properties

1. Introduction

Cadmium selenide belongs to II–VI compounds and it has been investigated for its potential applications in solar cells [1], photoconductors [2], thin film transistors [3], light emitting diodes [4] and gamma ray detectors [5]. SnSe belongs to the group of layer-type orthorhombic IV–VI compounds characterized by a strong anisotropy of the chemical bonds and physical properties. Tin selenide thin films have numerous applications as an efficient solar cell material [6], memory switching devices [7,8] and holographic recording system [9]. CdSe and SnSe have been studied in the form of both thin films [10,11] and single crystals [12,13]. CdSe is a narrow band semiconductor and its optical band gap is 1.74 eV [14], whereas the band gap of SnSe is 0.9 eV [15]. No study has been reported in the literature for $(CdSe)_X(SnSe)_{1-X}$ solid solution either in the form of thin films or single crystals and hence the study of mixed thin films of $Cd_{0.75}Sn_{0.25}Se$ is carried out. In this paper, we report the structural, optical, electrical and photoconducting properties of the vacuum deposited $Cd_{0.75}Sn_{0.25}Se$ thin films of various thicknesses.

2. Experimental

The bulk $Cd_{0.75}Sn_{0.25}Se$ material was synthesized in a quartz ampoule by mixing cadmium metal (AR grade), tin and selenium powders (Aldrich, 99.99%) in their stoichiometric ratio. The ampoule was evacuated to a pressure of 10^{-3} Pa, sealed and it was kept at the uniform temperature zone of the furnace. The temperature was gradually increased upto 900 °C and maintained in this temperature for a period of 10 h. The charged ampoule was rotated and shaked throughout this period to ensure complete mixing and then it was slowly cooled to room temperature in 20 h. The ampoule was broken, the sample was finely powdered, and again sealed in another quartz ampoule. The entire process of heating and soaking was repeated for homogeneous mixing. The synthesized final compound was analysed by X-ray diffraction (XRD) technique for their homogeneity and crystalline nature. The chemical analysis for the synthesized compound was carried out using atomic absorption spectrophotometer and found to contain Cd 38.3%, Sn 12.8% and Se 48.9%.

The thin films of $Cd_{0.75}Sn_{0.25}Se$ were deposited on glass substrates by vacuum deposition technique at room temperature (303 K). The substrates were thoroughly cleaned in a detergent solution and then in chromic acid and finally, cleaned using trichloroethylene. Double distilled water was used throughout in different stages of cleaning. The

* Corresponding author. Tel.: +91-463-233-3887; fax: +91-462-232-2973.
E-mail address: dppadiyan@rediffmail.com (D.P. Padiyan).

0254-0584/$ – see front matter © 2003 Elsevier B.V. All rights reserved.
doi:10.1016/j.matchemphys.2003.09.050

thin films of $Cd_{0.75}Sn_{0.25}Se$ were prepared in a vacuum coating unit (Hind Hivac Coating Unit, model 12-A4) at a pressure of 10^{-4} Pa using the synthesized $Cd_{0.75}Sn_{0.25}Se$ powder material. The coating was made at room temperature and the rate of coating was maintained at 5 nm s^{-1}. The films obtained in the above conditions were found to be reproducible. A quartz crystal film thickness monitor was used to measure the thickness of the films. Thin films thicknesses were also measured by forming interference fringes [16]. Thin films were prepared at three different thicknesses at room temperature namely 0.100, 0.168 and 0.182 μm.

The X-ray diffraction patterns for the synthesized powder sample and thin films were recorded with JEOL JDX 8030 X-ray diffractometer using Cu Kα radiation. The X-ray photoelectron spectra (XPS) were recorded with an ESCALAB MK II spectrometer (VG Scientific Ltd., UK) with Mg Kα radiation of energy 1253.6 eV. The optical transmittance spectra were recorded using UV-Vis-NIR spectrophotometer (Hitachi V-3400) in the wavelength region 400–2000 nm for the three samples having different thicknesses prepared at room temperature. The electrical conductivity measurements were studied by van der Pauw technique from 143 to 573 K. For electrical measurements, the ohmic contacts were made using high purity silver paste (Eltecks Corporation, Bangalore). The photoconductivity measurements were carried out using a halogen (100 W) lamp fed by a constant power supply.

3. Results and discussion

3.1. Structural properties

3.1.1. Powder sample

The powder XRD pattern recorded for the synthesized $Cd_{0.75}Sn_{0.25}Se$ powder sample is shown in Fig. 1 and it indicates that the material is polycrystalline in nature. The XRD peaks are indexed using a graphical method and also with the help of the software DICVOL91 [17,18]. The lattice constants are evaluated using ($h\,k\,l$) and 2θ values and refined with the help of the software UNITCELL [19]. The refined lattice parameters show that $Cd_{0.75}Sn_{0.25}Se$ crystallizes in the orthorhombic unit cell. The lattice constants are $a = 12.57 \pm 0.06$ Å, $b = 4.19 \pm 0.03$ Å and $c = 3.91 \pm 0.01$ Å [20]. Table 1 lists the 2θ, d, I, I/I_0 and $h\,k\,l$ values for $Cd_{0.75}Sn_{0.25}Se$ powder sample. Since there is no standard reported values are available for $Cd_{0.75}Sn_{0.25}Se$ mixed compound, residual factor is determined with reference to the calculated value using the formula

$$\text{residual factor},\ R = \sum \frac{|d_{obs} - d_{cal}|}{d_{obs}} \quad (1)$$

where d_{obs} is the actual experimental value and d_{cal} the least squares fitted value. The residual index obtained for $Cd_{0.75}Sn_{0.25}Se$ is 0.250. The low residue clearly indicates that the agreement between the experimental and least squares fitted values is good. In the synthesized powder

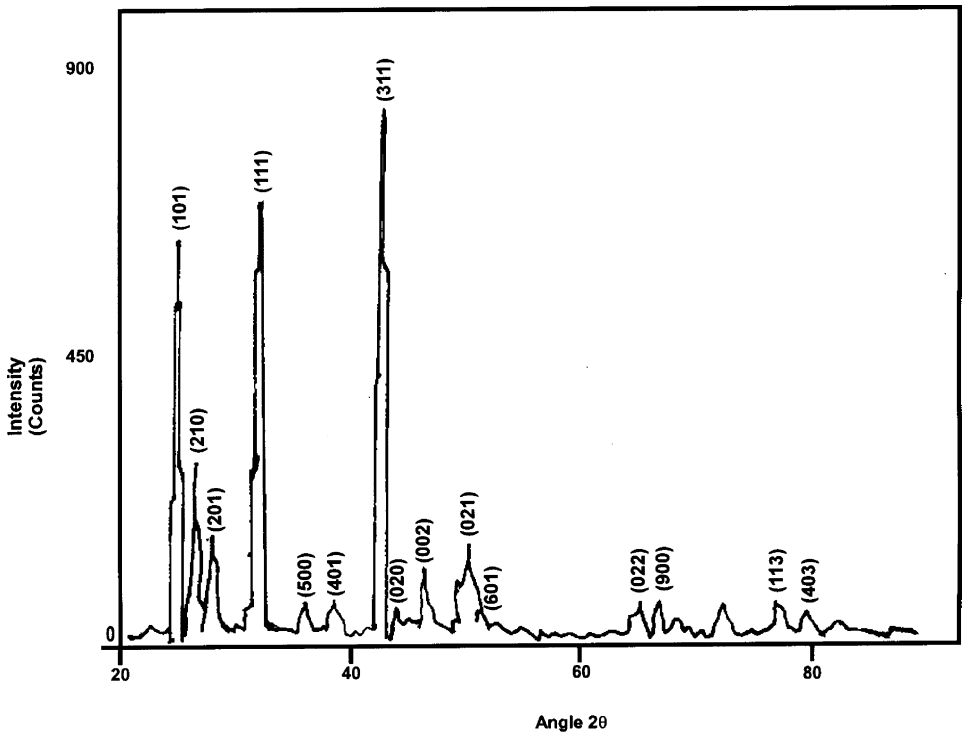

Fig. 1. XRD pattern of $Cd_{0.75}Sn_{0.25}Se$ powder material.

Table 1
XRD data for $Cd_{0.75}Sn_{0.25}Se$ powder material

Sl. no.	*hkl*	2θ (°)	*d* (Å) observed	*d* (Å) calculated	$I/I_0 \times 100$
1	(1 0 1)	24.2	3.675	3.731	79
2	(2 1 0)	25.6	3.477	3.487	36
3	(2 0 1)	27.3	3.264	3.319	24
4	(1 1 1)	31.4	2.847	2.787	86
5	(5 0 0)	35.4	2.534	2.515	11
6	(4 0 1)	38.1	2.360	2.449	11
7	(3 1 1)	42.3	2.135	2.361	100
8	(0 2 0)	43.7	2.070	2.095	9
9	(0 0 2)	46.1	1.967	1.954	17
10	(0 2 1)	49.1	1.854	1.846	15
11	(6 0 1)	50.0	1.823	1.847	22
12	(0 2 2)	65.2	1.430	1.429	10
13	(9 0 0)	66.7	1.401	1.397	11
14	(1 1 3)	77.1	1.236	1.238	11
15	(4 0 3)	79.8	1.201	1.203	9

XRD patterns of $Cd_{0.75}Sn_{0.25}Se$ the 2θ values for (1 1 1) peak is obtained at 31.4°, whereas for SnSe the 2θ value for (1 1 1) peak is obtained at 30.9° [20]. This shows that there is an evidence for SnSe phase in the synthesized $Cd_{0.75}Sn_{0.25}Se$ powder material.

3.1.2. Thin films

The $Cd_{0.75}Sn_{0.25}Se$ thin films prepared at room temperature did not give rise to any X-ray peak for all the three thicknesses. The absence of X-ray reflections reveals the poor crystalline nature of the films. However, annealing improves the crystallinity and few X-ray peaks are observed. Fig. 2 shows the XRD patterns recorded for the $Cd_{0.75}Sn_{0.25}Se$ thin films of thicknesses 0.100, 0.168 and 0.182 μm annealed at 300 °C for 2 h and their XRD data are displayed in Table 2. In Fig. 2a, two small X-ray peaks are observed at 2θ of 14.5 and 23.3°. They correspond to the X-ray reflection of (2 0 0) and (1 0 1) in comparison with the synthesized powder XRD data. Four well resolved X-ray peaks are observed for the film of thickness 0.168 μm as shown in Fig. 2b. Three peaks coincide well with the values of synthesized powder XRD data, while one peak could not be indexed. In Fig. 2c, for the film of thickness 0.182 μm, one X-ray peak is observed. Its *d* value agrees well with the standard powder XRD data.

Table 2
XRD data for $Cd_{0.75}Sn_{0.25}Se$ thin films annealed at 300 °C

Sl. no.	Thickness (μm)	2θ (°)	*I*	*d* (Å) measured	*d* (Å) standard	*hkl*
1	0.100	14.5	88	6.104	6.285	(2 0 0)
2	0.100	23.3	92	3.815	3.675	(1 0 1)
3	0.168	13.9	79	6.366	6.285	(2 0 0)
4	0.168	25.7	124	3.463	3.477	(2 1 0)
5	0.168	35.3	69	2.540	2.534	(5 0 0)
6	0.182	25.6	217	3.477	3.477	(2 1 0)

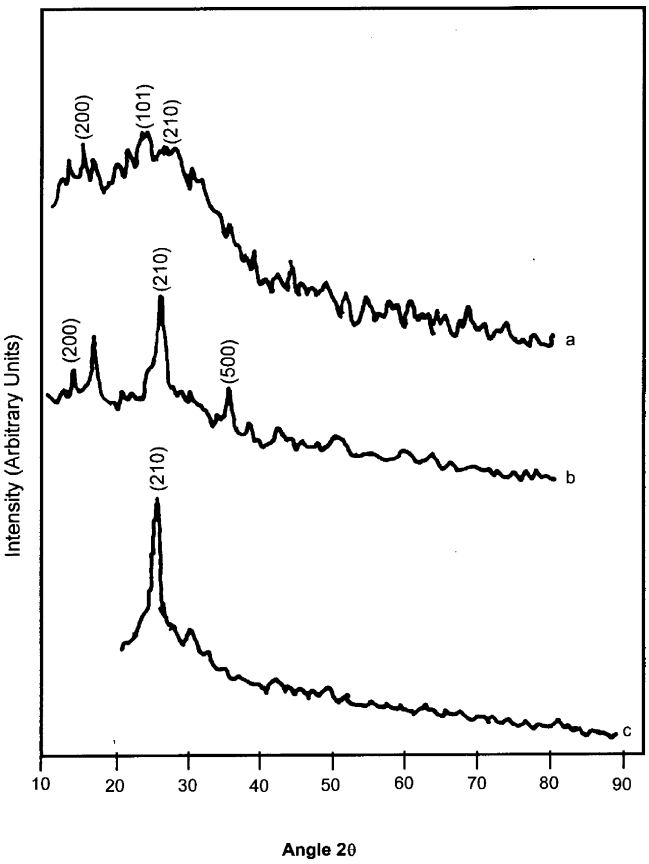

Fig. 2. XRD patterns of $Cd_{0.75}Sn_{0.25}Se$ thin films of thicknesses (a) 0.100, (b) 0.168 and (c) 0.182 μm, annealed at 300 °C.

3.2. XPS analysis

The XPS spectra of the vacuum deposited $Cd_{0.75}Sn_{0.25}Se$ thin films of thickness 0.182 μm prepared at room temperature is shown in Fig. 3. Quantitative analysis indicates that the films are rich in selenium and cadmium deficient and found to have Cd ∼ 35.1%, Sn ∼ 13.0% and Se ∼ 51.9% (in at.%). The actual chemical composition of the bulk and thin films is slightly different from the expected composition of $Cd_{0.75}Sn_{0.25}Se$. The chemical formula $Cd_{0.75}Sn_{0.25}Se$ represents the nominal composition of the sample.

The excess Se concentration found in evaporated $Cd_{0.75}Sn_{0.25}Se$ thin films could be related to the differences in the melting points of the constituents (Se: 217 °C, Sn: 231 °C and Cd: 320.9 °C), which would lead to a differential evaporation. The Se rich in $Cd_{0.75}Sn_{0.25}Se$ thin film is due to higher deposition rate. The change of film composition in CdSe from Cd rich to Se rich due to the increase in the deposition rate and source temperature has been reported by Chan and Hill [21]. The change of Cd rich to Se rich is also expected from the consideration of the vapour pressure curves for Cd and Se [22]. These curves show that the vapour pressure becomes increasingly rich in selenium as the source temperature increases.

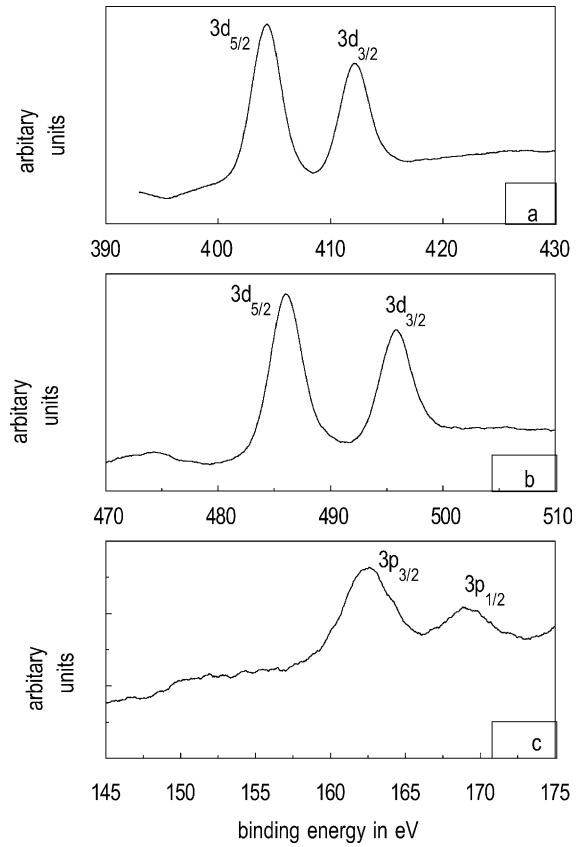

Fig. 3. Core level XPS spectra of (a) Cd, (b) Sn and (c) Se for $Cd_{0.75}Sn_{0.25}Se$ thin film of thickness 0.182 μm prepared at room temperature.

Presence of chemisorbed oxygen is observed in the surface layer of the films stored in the presence of atmospheric air. On sputtering the concentration of oxygen in the surface layer decreases. This is due to the well known fact of oxygen chemisorption mechanism in metal chalcogenide films. The measured peak positions of cadmium, tin and selenium

Table 3
XPS peak data for $Cd_{0.75}Sn_{0.25}Se$ thin films

Elements and subshells	Binding energy (eV) values for $Cd_{0.75}Sn_{0.25}Se$	Standard values (eV)
Cd ($3d_{5/2}$)	404.3	403.7
Cd ($3d_{3/2}$)	412.1	410.5
Sn ($3d_{5/2}$)	486.8	484.8
Sn ($3d_{3/2}$)	496.7	493.3
Se ($3p_{3/2}$)	158.1	161.9
Se ($3p_{1/2}$)	165.1	168.2

XPS peaks are given in Table 3. The binding energy values of the XPS peaks are calibrated with respect to carbon 1s line of the hydrocarbon contamination of spectrometer chamber as an internal standard of 284.0 eV. The shift in the peak position of Cd and Sn to higher energy side from their standard values may be due to the electrostatic charging. In Fig. 3b, the core level spectra of tin exhibits satellite feature in addition to the core level peaks. One satellite peak associated with the $3d_{5/2}$ tin line at 12.4 eV from the primary line is observed. There is a shift of selenium peak positions towards the lower energy side from their standard values. The observed shifts in the XPS peaks positions of Cd, Sn and Se is ascribed to electrostatic charging [23] and the oxygen chemisorption mechanism in metal chalcogenide thin films.

The separation energy of Cd doublet ($3d_{5/2}$–$3d_{3/2}$), tin doublet ($3d_{5/2}$–$3d_{3/2}$) and Se doublet ($3p_{3/2}$–$3p_{1/2}$) has increased from their standard values. The increase in the doublet separation could be due to the exchange splitting of their respective 3d/3p levels by the unpaired electrons [24]. The doublet separation is associated with multiplet splitting effect.

3.3. Optical properties

Fig. 4 shows the plot drawn between $(\alpha h\nu)^2$ versus $h\nu$ for the as-prepared $Cd_{0.75}Sn_{0.25}Se$ thin films prepared at

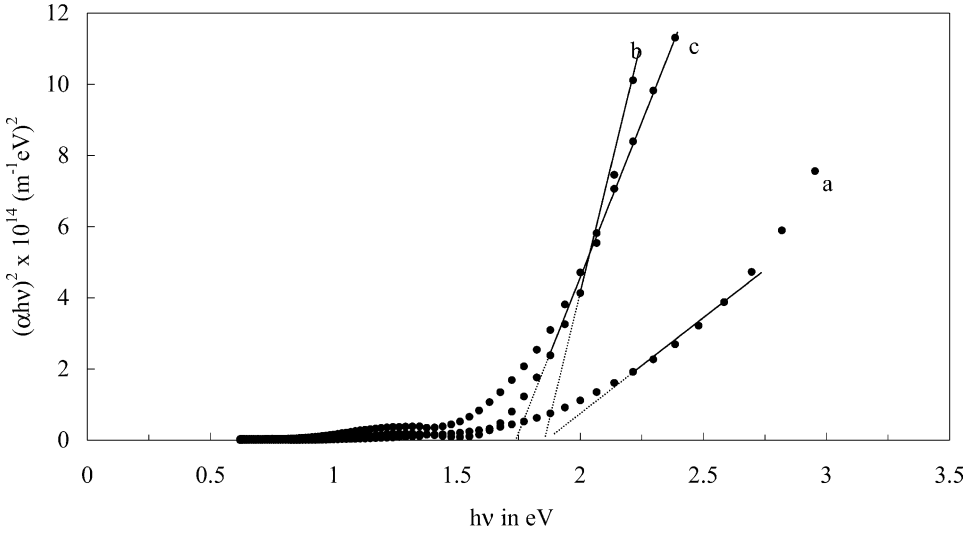

Fig. 4. A plot of $(\alpha h\nu)^2$ versus $h\nu$ for $Cd_{0.75}Sn_{0.25}Se$ thin film prepared at room temperature and of thicknesses (a) 0.100, (b) 0.168 and (c) 0.182 μm.

room temperature for the thicknesses of 0.100, 0.168 and 0.182 μm. The graph is linear in the strong absorption region near the fundamental absorption edge. Since the absorption coefficient is too large and it is measured at room temperature, the presence of the indirect band gap as in the case of the bulk sample is improbable [25,26]. The direct band gap energies evaluated from the *x*-axis intercept are 1.70 ± 0.05, 1.68 ± 0.04 and 1.67 ± 0.08 eV for the films of thicknesses 0.100, 0.168 and 0.182 μm, respectively.

A decrease in the band gap energy and the decrease in the optical transmittance is observed with increasing film thickness. The variation of band gap value with the film thickness has been reported by Shaalan and Müller [27] for their thermally evaporated cadmium selenide thin film and also by Pal et al. [28] for their vacuum evaporated polycrystalline cadmium selenide film.

3.4. Electrical properties

3.4.1. Below room temperature

The electrical conductivity of $Cd_{0.75}Sn_{0.25}Se$ thin films of thickness 0.182 μm prepared at room temperature is measured from 143 to 303 K and a plot of $\ln\sigma$ versus $10^3\,T^{-1}$ is shown in Fig. 5. The plot exhibits Arrhenius behaviour in the regions I and II in the temperature range 303–263 and 263–213 K, respectively. The activation energies calculated for these two regions are found to be 106 and 27.6 meV, respectively. Below 213 K, the variation of the conductivity with $10^3\,T^{-1}$ is not linear.

The Arrhenius plot can yield different levels, which are responsible for different donor and acceptor levels. The possibility of hopping conduction is analysed at very low temperatures. At low temperatures, all the trap states are filled and conduction occurs through the variable range hopping of the electrons in the localized states at Fermi levels.

The conductivity of the specimens exhibiting impurity conduction can be expressed as [29,30]

$$\sigma = \sigma_1 \exp\left(-\frac{\varepsilon_1}{kT}\right) + \sigma_2 \exp\left(-\frac{\varepsilon_2}{kT}\right) + \sigma_3 \exp\left(-\frac{\varepsilon_3}{kT}\right) \quad (2)$$

where $\sigma_1 > \sigma_2 > \sigma_3$ and $\varepsilon_1 > \varepsilon_2 > \varepsilon_3$. In Eq. (2), ε_1 is the activation energy for the ordinary conductivity due to the drifting of the charge carriers in the applied electric field, ε_2 the activation energy for the thermally assisted hopping and ε_3 the activation energy for the conductivity due to thermally assisted hopping to neighbouring sites from states that are close to the Fermi level, E_F. The third type of conductivity with activation energy ε_3 arises, if a band of localized states exists around E_F.

Fig. 5 shows that the $Cd_{0.75}Sn_{0.25}Se$ thin film exhibit, the first two types of conduction, namely (a) the ordinary conductivity due to the drifting of the charge carriers in the applied electric field (303–263 K) and (b) thermally assisted hopping (263–213 K). The absence of the third type of conductivity indicates the absence of localized band states around E_F. In these thin films below 263 K, the impurity conduction with activation energy ε_2 is dominant.

3.5. Photoconductivity

3.5.1. Steady state photoconductivity

The voltage dependence of the dark current and the photocurrents recorded at room temperature for $Cd_{0.75}Sn_{0.25}Se$ thin films of thickness 0.182 μm for different light intensity levels (600, 1800 and 3000 lx) are shown in Fig. 6. The dark conductivity and the total conductivity obtained for an applied voltage of 10 V for the light intensity of 3000 lx are 3.9×10^{-6} and $4.77 \times 10^{-6}\,S\,m^{-1}$, respectively. The photocurrent is obtained by subtracting the dark current from the total current. The dark current as well as the photocurrent increases linearly with the increase in voltage in the region studied (0–30 V). The experimental results show that the photoconductivity increases with the photoillumination and

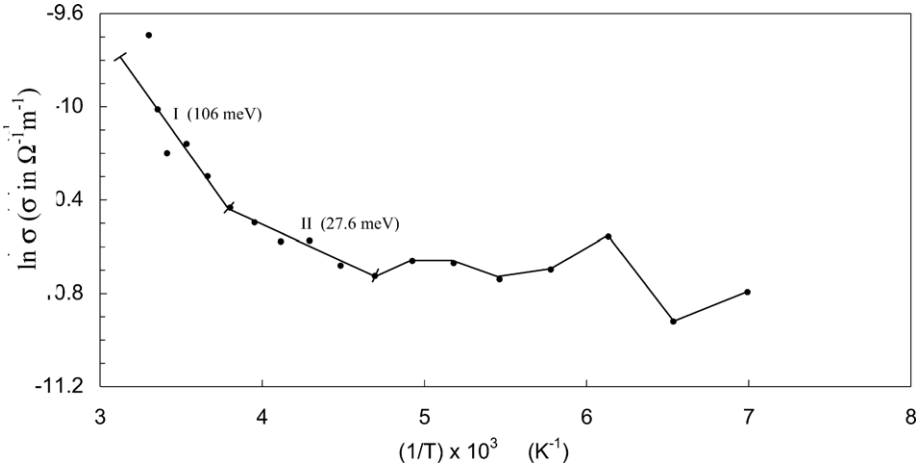

Fig. 5. A plot of $\ln\sigma$ versus $10^3\,T^{-1}$ for $Cd_{0.75}Sn_{0.25}Se$ thin film of thickness 0.182 μm in the temperature range 143–303 K.

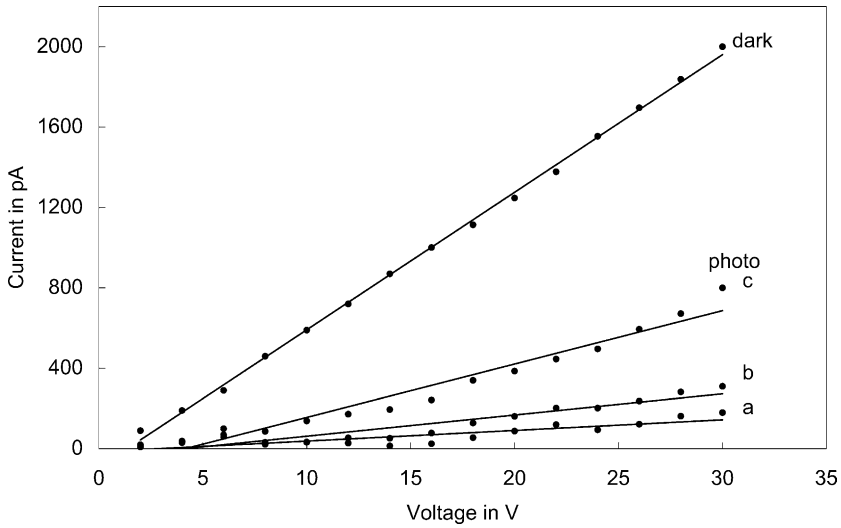

Fig. 6. Steady state photoconductivity for $Cd_{0.75}Sn_{0.25}Se$ thin film of thickness 0.182 μm measured at room temperature for the illumination levels of (a) 600, (b) 1800 and (c) 3000 lx.

it is due to the generation of free charge carriers. The slope of the current–voltage characteristics also increases with the increase in the illumination level F. The photoconductivities measured at 600, 1800 and 3000 lx are 2.11×10^{-7}, 2.18×10^{-7} and 8.69×10^{-7} S m^{-1}, respectively.

A plot is drawn between the photocurrent and illumination level on a logarithmic scale is shown in Fig. 7. The plot is a straight line indicating that there exists a linear relationship between the photocurrent and illumination level. The photocurrent follows a power law of the form

$$I_{ph} \propto F^{\gamma} \quad (3)$$

where γ is a constant and its value determine the recombination process [31]. For bimolecular recombination process, γ is equal to 0.5 and for monomolecular recombination process, the exponent γ is equal to 1. If γ lies between 0.5 and 1, it represents the existence of the continuous distribution of localized states. If $\gamma < 0.5$, it represents sublinear recombination and if $\gamma > 1$, it indicates supralinear recombination process. For $Cd_{0.75}Sn_{0.25}Se$, the value of γ is found to be 0.17 revealing the sublinear recombination mechanism. Devi and Prakash [32] have reported a similar sublinear recombination mechanism for their MgO–ZnO mixed system in polystyrene binder layer at higher light intensities.

3.5.2. Transient photoconductivity

The transient photoconductivity measurements are carried out by exposing these thin films using unpolarized white light and simultaneously the photocurrent is recorded. After reaching the steady state, the light is turned off and the current decay is followed. Fig. 8 shows the photodecay curve obtained at room temperature for the light intensity of 3000 lx.

The long photocurrent rise time and slow decay process observed in the $Cd_{0.75}Sn_{0.25}Se$ thin films is due to the presence of the deep localized gap states in these materials. The slow decay process is a function of time and it can be explained using the concept of differential lifetime τ_d [33].

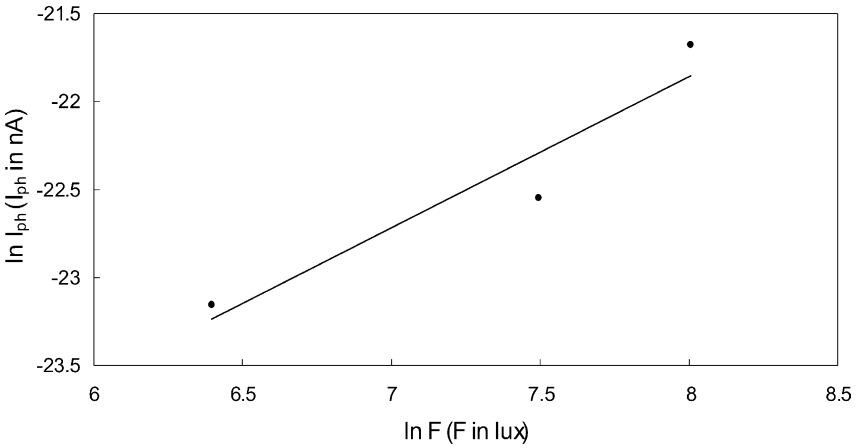

Fig. 7. A plot of $\ln I_{ph}$ versus $\ln F$ for $Cd_{0.75}Sn_{0.25}Se$ thin film of thickness 0.182 μm.

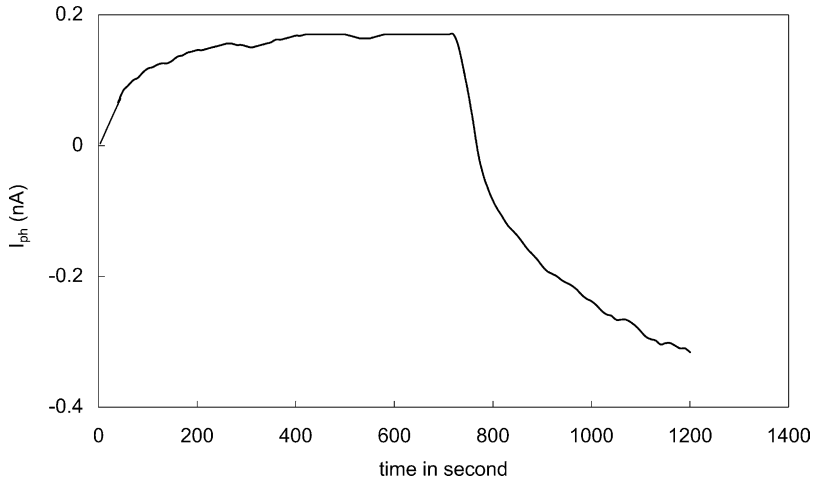

Fig. 8. Photodecay of $Cd_{0.75}Sn_{0.25}Se$ thin film of thickness 0.182 μm measured at room temperature for an illumination level of 3000 lx.

The lifetime for such a slow decay process can be written as

$$\tau_d = -\left[\frac{1}{I'_{ph}}\frac{dI_{ph}}{dt}\right]^{-1} \quad (4)$$

where I'_{ph} is the maximum photocurrent at $t = 0$.

The decay time observed for the $Cd_{0.75}Sn_{0.25}Se$ vacuum deposited thin films is found to be time dependent. In the case of non-exponential decay τ_d is not a constant and increases with time. At $t = 0$, τ_d gives the value of the carrier lifetime. In order to find the nature of decay τ_d is plotted with time t on a logarithmic scale is shown in Fig. 9. It shows that there is a linear relationship between $\ln \tau_d$ and $\ln t$, indicating that the decay is time dependent. The straight line obeys the power law of the form t^n, with

$$n = \frac{d(\ln \tau_d)}{d(\ln t)} \quad (5)$$

Moreover, the value of n is found to be 1.19.

The photosensitivity of the film is determined using the relation

$$S = \frac{\sigma_{ph}}{\sigma_d} \quad (6)$$

where σ_{ph} is the electrical conductivity of the sample when illuminated by light and σ_d is the dark conductivity. The photosensitivity of the film for an applied potential of 10 V are 0.05, 0.06 and 0.22 for 600, 1800 and 3000 lx, respectively. The photosensitivity increases with increase in the intensity of the light and the material is found to be weakly photosensitive.

The role of thickness in the photoconductivity behaviour is also studied. The dark current and the photocurrent increase with the increase of thickness of the $Cd_{0.75}Sn_{0.25}Se$ thin films. However, the steady state photoconductivity parameters are not varying with thickness.

The dark current after the light is switched off is lower than it was before illumination. Such a change in the dark conduction under the illumination is known as the

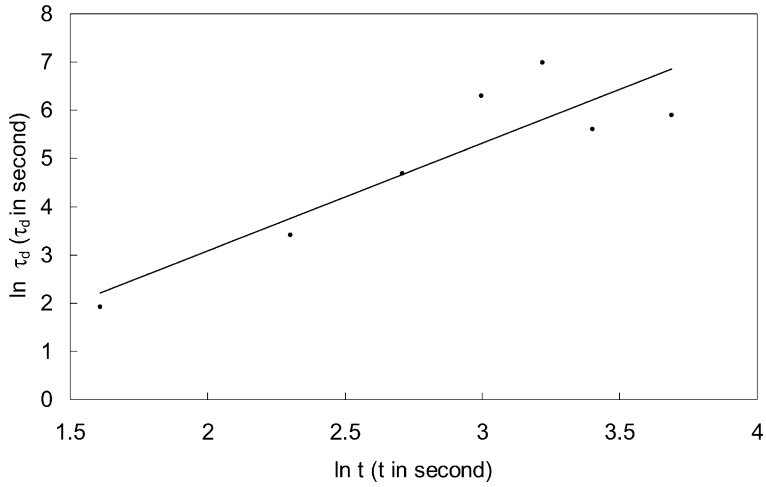

Fig. 9. A plot of $\ln \tau_d$ versus $\ln t$ for $Cd_{0.75}Sn_{0.25}Se$ thin film of thickness 0.182 μm showing the time dependent of photodecay.

Staebler–Wronski effect and is reported for doped and undoped a-Si:H films [34,35]. The decrease of dark current after the light is switched off is explained on the basis of photoassisted chemisorption of oxygen into the film, which would reduce the charge carrier mobility. Such an additional chemisorption and the corresponding reduction in the mobility would decrease the dark current value below that of the initial level when the illumination is stopped. Additionally, there would be a slight reduction in the internal field at the end of the illumination due to charge carriers trapped near the electrodes—an effect described as the photoelectret state [36,37], which would also contribute to a reduction in the value of the dark current when the illumination ceases.

4. Conclusions

The polycrystalline $Cd_{0.75}Sn_{0.25}Se$ thin films have been prepared at different thicknesses on glass substrates using vacuum deposition technique. The structural, electrical, optical and photoconducting properties are studied. The XRD pattern showed that $Cd_{0.75}Sn_{0.25}Se$ material crystallizes in orthorhombic crystal structure with lattice constants $a = 12.57 \pm 0.06$ Å, $b = 4.19 \pm 0.03$ Å and $c = 3.91 \pm 0.01$ Å. X-ray photoelectron spectroscopic analysis indicate that the vacuum deposited $Cd_{0.75}Sn_{0.25}Se$ thin films are rich in selenium and cadmium deficient. The films on storage in air adsorb oxygen, which is a common feature in metal chalcogenide films. The optical studies reveal that $Cd_{0.75}Sn_{0.25}Se$ has a direct band gap and the band gap energy varies with thickness. The observed electrical conductivity below room temperature shows that $Cd_{0.75}Sn_{0.25}Se$ thin films exhibit Arrhenius behaviour up to 213 K. Below 213 K, the $Cd_{0.75}Sn_{0.25}Se$ thin film samples exhibit metallic conduction and it is due to freezing of charge carriers. The photoconductivity studies showed the existence of the deep localized states and the $Cd_{0.75}Sn_{0.25}Se$ thin film are found to be weakly photosensitive. The photoconductivity measurements show that there is a linear dependence of photocurrents with the illumination intensity.

Acknowledgements

The authors thank the Department of Science and Technology, New Delhi for their financial support. We thank the Regional Sophisticated Instrumentation Centre at Indian Institute of Technology, Madras for XPS spectra measurements. One of the authors (AM) thanks the Management and the Principal of Mepco Schlenk Engineering College, Sivakasi for their encouragement.

References

[1] R.A. Boudrau, R.D. Rauh, Sol. Energy Mater. 7 (1982) 385.
[2] R.C. Kainthla, D.K. Pandya, K.L. Chopra, J. Electrochem. Soc. 127 (1980) 277.
[3] A. Van Calster, A. Vervaet, I. De Rycke, J. De Baets, J. Vanfleteren, J. Cryst. Growth 86 (1988) 924.
[4] J. Ren, K.A. Bowers, B. Sneed, D.L. Dreifus, J.W. Cook Jr., J.F. Schetzina, R.M. Kolbus, Appl. Phys. Lett. 57 (1990) 1901.
[5] M. Roth, Nucl. Instr. Meth. A 283 (1989) 291.
[6] D.I. Bletskan, I.F. Kopinets, P.P. Pogorsh, E.N. Salkora, D.V. Chepor, Kristallografiya 20 (1978) 1008.
[7] T.S. Rao, B.K.S. Ray, A.K. Chaudhurai, Thin Solid Films 165 (1988) 257.
[8] C.R. Baxter, W.D. McLennan, J. Vac. Sci. Technol. 12 (1975) 110.
[9] M. Rodot, Acta Electron. 18 (1975) 345.
[10] S. Eriksson, T. Gruszecki, P. Carlsson, B. Holmström, Thin Solid Films 269 (1995) 14.
[11] T. Terada, J. Phys. D 4 (1971) 1991.
[12] A. Burger, M. Roth, J. Cryst. Growth 67 (1984) 507.
[13] O.P. Agnihotri, A.K. Jain, B.K. Gupta, J. Cryst. Growth 46 (1979) 491.
[14] D.R. Lide, H.P.R. Frederikse (Eds.), CRC Handbook of Chemistry and Physics, CRC Press, USA, 1994, pp. 12–95.
[15] V.P. Bhatt, K. Gireesan, C.F. Desai, Cryst. Res. Technol. 24 (1989) 187.
[16] A. Goswami, Thin Film Fundamentals, New Age International (P) Ltd., New Delhi, 1996.
[17] D. Louër, M. Louër, J. Appl. Cryst. 5 (1972) 271.
[18] A. Boultif, D. Louër, J. Appl. Cryst. 24 (1991) 987.
[19] T.J.B. Holland, S.A.T. Redfern, Mineral. Mag. 61 (1997) 65.
[20] D. Pathinettam Padiyan, A. Marikani, Cryst. Res. Technol. 37 (2002) 1241.
[21] D.S.H. Chan, A.E. Hill, Thin Solid Films 38 (1976) 163.
[22] K.G. Gunther, in: J.C. Anderson (Ed.), The Use of Thin Films in Physical Investigations, Academic Press, London, 1966.
[23] C.D. Wagner, W.M. Riggs, L.E. Davis, T.F. Moulder, G.E. Muilenberg, Handbook of X-ray Photoelectron Spectroscopy, Perkin-Elmer, Norwalk, CT, 1978, p. 182.
[24] P. Selvam, B. Viswanathan, V. Srinivasan, J. Less Common Met. 161 (1990) 1.
[25] K.J. John, B. Pradeep, E. Mathai, J. Mater. Sci. 29 (1994) 1581.
[26] R.A. Smith, Semicondutors, 1st ed., Cambridge University Press, Cambridge, 1959.
[27] M.S. Shaalan, R. Müller, Solar Cells 28 (1990) 185.
[28] U. Pal, D. Samanta, S. Ghorai, A.K. Chaudhuri, J. Appl. Phys. 74 (10) (1993) 6368.
[29] D.S.H. Chan, A.E. Hill, Thin Solid Films 38 (1976) 163.
[30] H.M. Rosenberg, The Solid State, 3rd ed., Oxford University Press, Oxford, 1989, p. 285.
[31] A. Rose, Concepts in Photoconductivity and Allied Problems, Wiley–Interscience, New York, 1963, p. 34.
[32] S. Devi, S.G. Prakash, Pramana-J. Phys. 39 (1992) 145.
[33] W. Fuhs, D. Meyer, Phys. Status Sol. (a) 24 (1974) 275.
[34] D.L. Staebler, C.R. Wronski, Appl. Phys. Lett. 31 (1977) 292.
[35] J.H. Yoon, M.S. Kim, Ch. Lee, J. Non-Cryst. Solids 114 (1989) 636.
[36] M.T.S. Nair, P.K. Nair, R.A. Zingaro, E.A. Meyers, J. Appl. Phys. 74 (1993) 1879.
[37] P.K.C. Pillai, R. Nath, P.K. Nair, Ind. J. Pure Appl. Phys. 16 (1978) 698.